CSCanada
Advances in Petroleum Exploration and Development
Vol. 3, No. 1, 2012, pp. 1-10
DOI:10.3968/j.aped.1925543820120301.152

ISSN 1925-542X [Print]
ISSN 1925-5438 [Online]
www.cscanada.net
www.cscanada.org

Hybrid Forecasting Methods for Multi-Fractured Horizontal Wells: EUR Sensitivities

Morteza Nobakht[1,*]; Christopher Clarkson[1]

[1]University of Calgary, 2500 University Dr. NW, Calgary, Alberta, T2N 1N4, Canada.
*Corresponding author.

Received 16 January 2012; accepted 28 February 2012

Abstract

In this paper, the sensitivity of expected ultimate recovery (EUR) for horizontal wells with multiple fractures to decline exponent is studied using the simplified forecasting method introduced by Nobakht et al.[1]. This is very important from the reserves evaluation perspective due to uncertainty in decline exponent, *b*. This uncertainty is caused by many factors like desorption and reservoir/completion heterogeneity. It is found that in case of time-based forecast (duration of forecast is specified), the ratio of EURs for two different specified values of decline exponent depends on the ratio of economic life time of a well to the duration of linear flow. On the other hand, this EUR ratio depends on the ratio of rate at the end of linear flow to economic rate limit for economic limit-based forecast (economic rate limit is specified).

Key words: EUR sensitivities; Multi-fractured horizontal wells; Hybrid forecasting methods

Nobakht, M., & Clarkson, C.R. (2012). Hybrid Forecasting Methods for Multi-Fractured Horizontal Wells: EUR Sensitivities. *Advances in Petroleum Exploration and Development*, *3*(1), 1-10. Available from: URL: http://www.cscanada.net/index.php/aped/article/view/j.aped.1925543820120301.152
DOI: http://dx.doi.org/10.3968/j.aped.1925543820120301.152

Nomenclature

A = Drainage area, ft^2
b = Hyperbolic decline exponent, dimensionless
b' = Intercept of inverse gas rate versus square root of time plot, 1/(Mscf/D)
B_g = Gas formation volume factor, ft^3/scf
c_g = Gas compressibility, psi^{-1}
c_t = Total compressibility, psi^{-1}
D_{elf} = Decline rate at the end of linear flow, 1/day
D_i = Decline rate at the start of hyperbolic forecast, 1/day
EUR = Expected ultimate recovery, Mscf
h = Net pay thickness, ft
k = Permeability, mD
m = Slope of inverse gas rate versus square root of time plot, day$^{1/2}$/Mscf
n = The ratio of the rate at the end of linear flow to the economic rate limit
$OGIP$ = Original gas-in-place, Mscf
p = Pressure, psi
p_i = Initial pressure, psi
p_{pi} = Pseudopressure at initial pressure, psi^2/cp
p_{pwf} = Pseudopressure at flowing pressure, psi^2/cp
p_{wf} = Flowing pressure, psi
q = Gas rate, Mscf/D
q_i = Gas rate at the start of hyperbolic forecast, Mscf/D
q_D = Dimensionless rate, dimensionless
q_{Dd} = Dimensionless rate, dimensionless
$(q_{Dye})_{elf}$ = Dimensionless rate at the end of linear flow, dimensionless
q_{elf} = Gas rate at the end of linear flow, Mscf/D
Q = Gas cumulative production, Mscf
Q_{elf} = Gas cumulative production at the end of linear flow, Mscf
ΔQ = Volume of gas produced between the end of linear flow and end of forecast, Mscf
S_g = Gas saturation, fraction
t = Economic life of a well, days
t_{Dye} = Dimensionless time, dimensionless
$(t_{Dye})_{elf}$ = Dimensionless time at the end of linear flow, dimensionless
t_{elf} = Duration of linear flow, days
T = Reservoir temperature, $\circ R$

x_e = Reservoir width, ft
x_f = Fracture half-length, ft
y_e = Reservoir length, ft
Z = Gas compressibility factor

Greek Symbols

γ_g = Reservoir gas specific gravity (air=1)
ϕ = Porosity, fraction
μ_g = Gas viscosity, cp

INTRODUCTION

Shale gas reservoirs have become a significant source of gas supply in North America owing to the advancement of drilling and stimulation techniques to enable commercial development. Production analysis and forecasting of shale gas wells is difficult due to complex reservoir behavior (ex. ultra-low matrix permeability, dual porosity or dual permeability behavior, heterogeneities at all scales, stress-dependent porosity and permeability etc.) and complex wellbore architectures and stimulation and completion methods. The most popular method for exploiting shale gas reservoirs today is the use of long horizontal wells completed with multiple-fracturing stages; the resulting, often complex, hydraulic fracture network can impart further complexity for production analysis and forecasting. Although rigorous methods to account for reservoir and hydraulic fracture network complexities in production data analysis and forecasting using numerical modeling approaches have been proposed[2], it is desirable to seek simpler methods for analysis and forecasting that can be used more routinely by the reservoir engineer.

Simple empirical methods such as Arps' decline curve method[3] have been used historically to forecast multi-fractured horizontal wells (MFHW). The Arps' method, where the rate profile is described by a constant b-value, is limited to cases where operating conditions are not changing and the well is in boundary-dominated flow. For tight formations, the transient flow may continue for a long time and therefore, Arps' decline may not be applicable to these formations. Stright and Gordon[4] studied the production decline curves of three low-permeability gas wells in Piceance basin and found that linear flow equations can be used to approximate long term production in these wells. To forecast rates during boundary-dominated flow, they suggested switching from the forecast based on linear flow projection to exponential decline when decline rate reaches a pre-determined value. Maley[5] studied the linear flow in tight formations and concluded that linear flow can be modeled using Arps decline using b = 2. Hale[6] analyzed the monthly production rates of more than 6000 hydraulically fractured gas wells located in low-permeability reservoirs. He compared exponential forecasting, logarithmic forecasting and linear flow forecasting. However, no method was defined on how to forecast rates during boundary-dominated flow. Wattenbarger et al.[7] also focused on linear flow as the flow regime that lasts for a long time in tight gas reservoirs. They used the reservoir geometry shown in Fig.1 and developed general solutions for linear flow. They proposed to use the constant productivity index during boundary-dominated flow. Kupchenko et al.[8] proposed using b = 2 to forecast during linear flow and switch to b = 0.5 during boundary-dominated flow. They determined the end of linear flow for a hydraulically-fractured (vertical) well, located in square reservoir geometry, based on assumed value for porosity and some assumption for gas properties. The power-law and the stretched exponential decline are new empirical methods introduced by Ilk et al.[9] and Valkó[10], respectively. These methods account for changing b-value with time. Due to number of parameters in these techniques, they produce non-unique forecasts[11]. Recently, a semi-empirical method was developed that models changing b-value with time in multi-fractured horizontal wells with unequal fracture half-lengths and/or non-uniform fracture spacing along horizontal well[12].

Recognizing that the flow regime most often observed in multi-fractured horizontal wells is linear flow, Nobakht et al.[1] developed a simplified forecasting method for horizontal wells with multiple fractures in tight/shale gas reservoirs. This semi-empirical method was developed assuming that the transient linear flow is the dominant flow-regime in horizontal wells with multiple fractures, which is a reasonable assumption. This flow regime may continue for several years, and will ultimately become boundary-dominated flow at much later times. This method combines the linear flow transient period with hyperbolic decline during boundary-dominated flow. The slope of the inverse gas rate versus square root of time plot is used to yield a forecast for transient linear flow and then applied the Arps' hyperbolic decline for boundary-dominated flow. A method for estimating the start of boundary-dominated flow was provided that does not rely on an estimate of matrix permeability (often elusive for tight formations because of the difficulty in measurement) or fracture half-length.

In this paper, first, the above-mentioned simplified forecasting method is briefly reviewed. Secondly, it is shown that for gas production under constant flowing pressure in a volumetric reservoir, at some point during depletion the decline exponent starts to deviate from 0.5. The time of this transition is correlated to permeability, porosity, gas properties and reservoir width. Thirdly, it is shown that ignoring this transition from b = 0.5 for forecasting is not affecting the forecast practically. Finally, the sensitivity of expected ultimate recovery to b-value is studied for both time-based and economic-limit based forecasts.

1. REVIEW OF SIMPLIFIED FORECASTING METHOD

The base reservoir geometry, for which the simplified forecasting method was developed, is shown in Fig. 1. The well is at the center of a rectangular reservoir and the fracture extends all the way to the lateral boundaries of the reservoir. This geometry was first used by Wattenbarger et al.[7] for modeling linear flow in tight gas reservoirs. This base geometry was chosen as it is reasonable to assume that drainage beyond the stimulated region is insignificant for ultra-low matrix permeability reservoirs. The constant flowing pressure solution was used by Nobakht et al.[1] for linear flow analysis, as in practice, tight gas and shale gas wells are produced under high drawdown to maximize production. The forecasting procedure using this simplified method of Nobakht et al.[1] follows the 7 steps below:

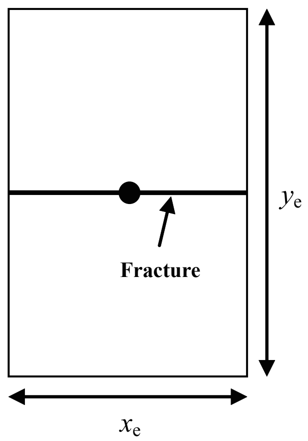

Figure 1
A Hydraulically Fractured Vertical Well in the Center of a Rectangular Reservoir

Step 1. Plot $\frac{1}{q}$ versus $\sqrt{t}$, where q is gas rate and t is time, on Cartesian coordinates and place a line through the data corresponding to linear flow. Determine the slope, *m,* of this line and its intercept, *b'*. Linear flow can be recognized independently using semi-log derivative analysis.

Step 2. Specify a value for drainage area.

Step 3. Calculate the duration of linear flow, t_{elf}.

$$t_{elf} = \left[\frac{Ah(\phi \mu_g c_t)_i m\ (p_{pi} - p_{pwf})}{200.6T} \right]^2 \quad (1)$$

In this equation, A is the drainage area, h is the net pay thickness, ϕ is the reservoir porosity, μ_g is gas viscosity, c_t is total compressibility, subscript "i" refers to initial reservoir conditions, p_{pi} and p_{pwf} are pseudopressures at initial pressure and flowing pressure, respectively and T is the reservoir temperature. It should be noted that Eq. (1) is derived for field units.

Step 4. Calculate the production rate at the end of the linear flow period, q_{elf}.

$$q_{elf} = \frac{1}{m\sqrt{t_{elf}} + b'} \quad (2)$$

Step 5. Calculate the decline rate at the end of the linear flow period, D_{elf}.

$$D_{elf} = \frac{1}{m\sqrt{t_{elf}} + b'} \times \frac{m}{2\sqrt{t_{elf}}} \quad (3)$$

Step 6. Forecast rates for $t \le t_{elf}$ using the following equation:

$$q = \frac{1}{m\sqrt{t} + b'} \quad (4)$$

Step 7. Assume a value for decline exponent, b, and use Eq. (5) to forecast rates for $t > t_{elf}$.

$$q = \frac{q_{elf}}{\left[1 + bD_{elf}(t - t_{elf})\right]^{1/b}} \quad (5)$$

In the preceding equations, b and b' are in no way related. b' is the intercept of inverse gas rate versus square root of time plot whereas b is the hyperbolic decline exponent. Although this forecasting procedure was developed for the reservoir geometry shown in Fig.1, it can be used to forecast rates for horizontal well with multiple fracture system shown in Fig. 2 using the area of stimulated reservoir volume (SRV) as the input to the simplified method instead of drainage area[1].

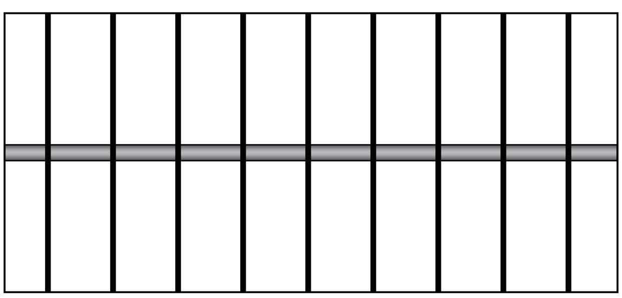

Figure 2
Schematic of a Homogeneous Multi-Fractured Horizontal Well Completion

2. DECLINE EXPONENT (*b*-VALUE)

This forecasting procedure requires a decline exponent to forecast rates during boundary-dominated flow (Step 7). It is well documented in the literature that for volumetric gas reservoirs $b = 0.5$ can be used in hyperbolic decline. Therefore, $b = 0.5$ is a good number to be used for tight gas. However, for shale gas reservoirs, depending on operating conditions and the shape of desorption isotherm, desorption can cause the b value to be above 0.5. b value larger than 0.5 is also expected in multi-layer reservoirs with no cross flow.

This forecasting method with $b = 0.5$ is only applicable to horizontal wells with homogeneous completions (i.e., the fractures have the same length)[11]. Ambrose et al.[11] proposed that for a heterogeneous completion, where the fracture lengths are not the same (Fig. 3), the system needs to be divided into sub-components and then for each sub-component, the simplified forecasting method of Nobakht et al.[1] can be applied. It was shown that for a volumetric gas reservoir after the first two fractures start to interfere, the decline exponent value starts to deviate from $b = 2$ and when the whole system is in boundary-dominated flow the decline exponent value reaches $b = 0.5$. Using some real data, Ambrose et al.[11] showed that Nobakht et al. method[1] with a decline exponent between 0.5 and 2 (after the end of linear flow) can be used to forecast rates from heterogeneous completions. The decline exponent that should be used depends on the completion geometry. This shows that when using the simplified forecasting method for shale gas reservoirs, there might be uncertainties in decline exponent and therefore, it is important to study the relative impact of b-value used after the end of linear flow on long-term production forecast for linear-flow dominated wells.

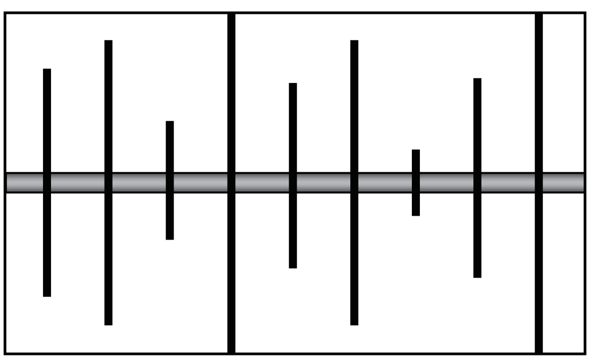

Figure 3
Schematic of a Heterogeneous Multi-Fractured Horizontal Well Completion

2.1 Evolution of Decline Exponent During Depletion

It is observed in the literature that for constant flowing pressure production from a single layer volumetric gas reservoir, the decline exponent during boundary-dominated flow is going to deviate from $b = 0.5$ and eventually reduces to $b = 0$[1,13]. It is important to find the time that this deviation starts and determine if it practically affects the expected ultimate recovery (EUR) calculated from Arps' decline. In this section, this time is determined for the reservoir geometry shown in Fig. 1. First, the constant-pressure type curve for this reservoir geometry was developed using the linear flow solution for a slightly compressible fluid during linear flow[7] and hyperbolic decline with $b = 0.5$ during boundary-dominated flow. The plotting format for this type curve, shown in Fig. 4, is $q_{Dd} = \frac{y_e}{x_e} q_D$ against t_{Dye} [7], where:

$$q_D = \frac{141.2 qB\mu}{kh\left(p_i - p_{wf}\right)} \tag{6}$$

$$t_{Dye} = \frac{0.00633kt}{\phi\mu c_t y_e^2} \tag{7}$$

The manner in which the type curve is generated is presented in Appendix A. This plotting format gives only one type curve for geometry shown in Fig. 1 rather than families of type curves with different values of $\frac{x_f}{y_e}$ [7]. As shown in Appendix A, $t_{Dye} = 0.0625$ at the end of the linear flow period (i.e., at $t = t_{elf}$).

To calculate the time that the decline exponent starts to deviate from $b = 0.5$, a total number of 10 simulation cases were generated for constant flowing pressure condition. The input data for the numerical simulation cases are given in Table 1. The blank cells in this table indicate that the value for that parameter is the same as that of Case 1. The rate versus time data points for these cases was transformed to q_{Dd} versus t_{Dye} format and plotted on the type curve. Fig. 4 also shows this data plotted on the type curve for Cases 1–5. This figure shows that for all cases, the b value starts to gradually decrease from $b = 0.5$ around $t_{Dye} = 0.4$. As $t_{Dye} = 0.0625$ at $t = t_{elf}$, it can be concluded that the b value starts to deviate from $b = 0.5$ around $t = 6t_{elf}$. The simulated data during linear flow do not fall on the half-slope part of the type curve in Fig. 4. This is because we simply used time instead of pseudo-time for plotting the data on the type curve[14,15].

Table 1
Input Parameters Used for Numerical Simulation for Different Cases, the Blank Cells in this Table Indicate that the Value for that Parameter is the Same as that of Case 1

Case	1	2	3	4	5	6	7	8	9	10
p_i (psi)	2,000						1,000	4,000		
T (°F)	120									
h (ft)	100									
ϕ(%)	10									
S_g (%)	100									
γ_g	0.65									
p_{wf} (psi)	200								500	1,000
x_f (ft)	250									
x_e (ft)	500									
y_e (ft)	5,000				10,000	2,500				
k (md)	1	0.5	2	4						

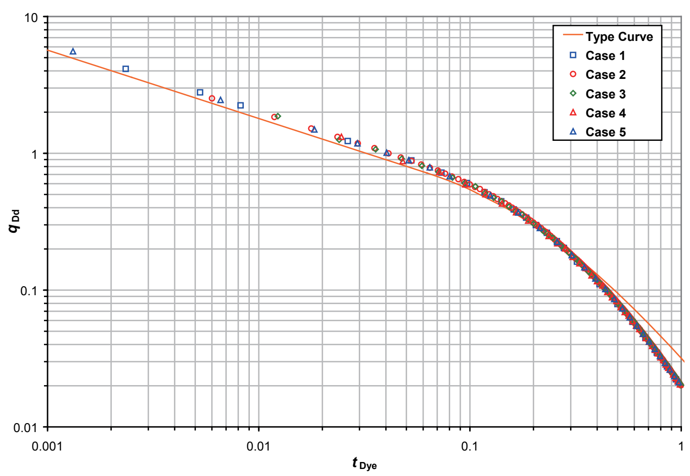

Figure 4
The Rate Versus Time Data Points for Cases 1–5 Plotted on the q_{Dd} Versus t_{Dye} Type Curve

To investigate if the gradual deviation of decline exponent from $b = 0.5$ affects the EUR, the following assumptions are made to simplify the problem:

1. The gas is ideal ($Z = 1$). Using the definition of gas compressibility, this assumption leads to:

$$c_g = \frac{1}{p} - \frac{1}{Z}\frac{dZ}{dp} = \frac{1}{p} \quad (8)$$

2. Gas viscosity is not changing with pressure. Using the definition of pseudopressure and ideal gas assumption,

$$p_{pi} = 2\int \frac{p}{\mu_g Z} dp = \frac{2}{\mu_{gi}} \int p dp = \frac{p_i^2}{\mu_{gi}} \quad (9)$$

3. Total compressibility is dominated by gas compressibility, i.e.,

$$c_t = S_g c_g \quad (10)$$

4. Pseudopressure at the constant flowing pressure is negligible compared to that at the initial pressure. In other words,

$$p_{pi} - p_{pwf} \approx p_{pi} \quad (11)$$

5. The intercept of inverse gas rate versus square root of time plot is ignored. In other words, the rate can be calculated using the following equation during linear flow period:

$$q = \frac{1}{m\sqrt{t}} \quad (12)$$

Using Eq. (12), the cumulative production at the end of linear flow (i.e., $t = t_{elf}$) is:

$$Q_{elf} = \int_0^{t_{elf}} q dt = \int_0^{t_{elf}} \frac{1}{m\sqrt{t}} dt = \frac{2}{m}\sqrt{t_{elf}} \quad (13)$$

Combining Eqs. (1), (8)–(11) and (13) and using the definition of gas formation volume factor $B_{gi} = \dfrac{0.0282 Z_i T}{p_i}$ with Z_i=1 (ideal gas assumption),

$$Q_{elf} = 0.282 OGIP \tag{14}$$

where OGIP is the original gas-in-place in Mscf. This means that under assumptions mentioned above, 28% of the total gas in the reservoir geometry shown in Fig. 1 is produced during linear flow.

The relationship between cumulative production and time for hyperbolic decline is as follows:

$$Q = \frac{q_i}{(1-b)D_i}\left[1-(1+bD_i t)^{1-\frac{1}{b}}\right] \tag{15}$$

where q_i is the production rate at the start of the hyperbolic forecast period, b is the hyperbolic decline exponent, D_i is decline rate corresponding to q_i and t is time since the start of the hyperbolic forecast. Since hyperbolic forecast starts after the end of linear flow, we will use the hyperbolic decline equation in the form shown in Eq. (16), which is obtained from Eq. (15) by re-initializing the time at $t = t_{elf}$:

$$\Delta Q = \frac{q_{elf}}{(1-b)D_{elf}}\left[1-\left(1+bD_{elf}(t-t_{elf})\right)^{1-\frac{1}{b}}\right] \tag{16}$$

In this equation, ΔQ is the volume produced during boundary-dominated flow using hyperbolic decline. Using q_{elf} and D_{elf} from Eq. (2) and Eq. (3) respectively (with b' = 0), the volume produced between $t = t_{elf}$ and $t = 6t_{elf}$ (i.e., when the decline exponent starts to deviate from b = 0.5) using b = 0.5 becomes:

$$\Delta Q\ (b = 0.5) = \frac{2.22\sqrt{t_{elf}}}{m} \tag{17}$$

Combining Eqs. (17) and (B-4),

$$\Delta Q\ (b = 0.5) = 0.313 OGIP \tag{18}$$

This shows that 31% of the original gas-in-place is produced between $t = t_{elf}$ and $t = 6t_{elf}$ using hyperbolic decline with b = 0.5. In other words, almost 60% of the total gas will be produced by the time the decline exponent starts to deviate from b = 0.5.

As shown in Appendix B, 25% of the total gas will be recovered after $t = 6t_{elf}$ using b = 0.5 to forecast for infinite time, whereas 12% of the total gas will be produced after $t = 6t_{elf}$ using exponential decline. Therefore, the volume of gas produced after $t = 6t_{elf}$ is between 12% and 25% of the original gas-in-place, as there is a transition from b = 0.5 to b = 0. This shows that for all practical purposes, we can ignore the change in decline exponent with time for $t \geq 6t_{elf}$.

Notes:

- Although the calculations presented above and in Appendix B are based on ideal gas assumption (Z = 1), they are valid for cases where Z is not changing drastically with pressure.
- The cumulative productions at different times presented above and in Appendix B are obtained based on the duration of linear flow from Eq. (1). Although it is reported in the literature that Eq. (1) is an approximation for the duration of linear flow[16–18], it is used for simplicity in this study.

3. SENSITIVITY OF FORECAST TO *b*-VALUE

As mentioned in the previous section, after the fractures start to interfere in a multi-fractured horizontal well, the decline exponent can vary between 0.5 and 2 due to different fracture lengths and/or unequal fracture spacing along the horizontal well (heterogeneous completions). The simplified forecasting procedure can be used to investigate the sensitivity of EUR to decline exponent, b, which is being used for forecasting during boundary-dominated flow.

3.1 EUR Based upon Time

Eq. (16) shows the volume produced after the end of linear flow according to a hyperbolic decline forecast. To obtain the expected ultimate recovery (EUR) at the end of the forecast (when $t > t_{elf}$), the volume produced using Eq. (16) can be added to the cumulative production at the end of linear flow calculated from Eq. (13). Combining Eqs. (2), (3), (13) and (16):

$$EUR = \frac{2\sqrt{t_{elf}}}{m}\left[1+\frac{1}{1-b}\left[1-\left(1+\frac{b}{2}\left(\frac{t}{t_{elf}}-1\right)\right)^{1-\frac{1}{b}}\right]\right] \tag{19}$$

Here, t is the economic life of the well. Using Eq. (19), it can be shown that the ratio between EUR values obtained for two different values of decline exponent depends on the value of $\dfrac{t}{t_{elf}}$, given that the two decline exponents are specified.

$\dfrac{EUR(b = 1.3)}{EUR(b = 0.5)}$ and $\dfrac{EUR(b = 0.8)}{EUR(b = 0.5)}$ versus $\dfrac{t}{t_{elf}}$ are shown in Fig. 5 and Fig. 6, respectively. These plots can be used to study the sensitivity of forecast to the value of decline exponent. For example, it can be seen from Fig. 6 that for $t = 30t_{elf}$, EUR for b = 0.8 is almost 20% higher than EUR for b = 0.5. It should be noted that b = 0.5 is for homogeneous completion, b = 0.8 is for slightly heterogeneous completion and b = 1.3 is for very heterogeneous completion[11].

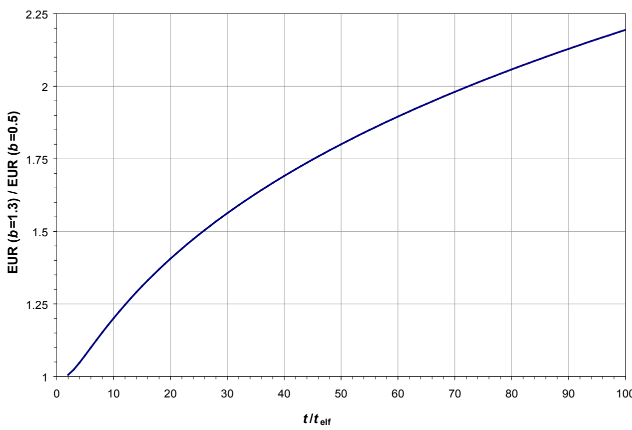

Figure 5
Plot of $\frac{EUR(b=1.3)}{EUR(b=0.5)}$ Versus $\frac{t}{t_{elf}}$

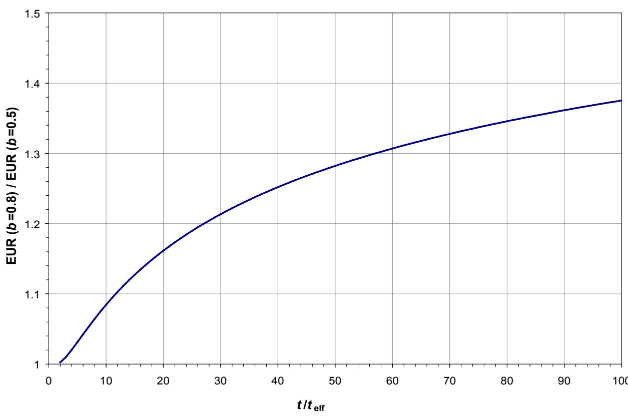

Figure 6
Plot of $\frac{EUR(b=0.8)}{EUR(b=0.5)}$ Versus $\frac{t}{t_{elf}}$

3.2 EUR Based upon Economic Limit

When economic limit, q_f, is known, the volume produced using hyperbolic decline is calculated using the following equation:

$$Q = \frac{q_i^b}{(1-b)D_i}\left[q_i^{1-b} - q_f^{1-b}\right] \tag{20}$$

Therefore, the volume produced during boundary-dominated flow ΔQ for hyperbolic decline is:

$$\Delta Q = \frac{q_{elf}^b}{(1-b)D_{elf}}\left[q_{elf}^{1-b} - q_f^{1-b}\right] \tag{21}$$

Using q_{elf} and D_{elf} from Eq. (2) and Eq. (3) respectively (with $b' = 0$) and assuming n is the ratio of the rate at the end of linear flow to the economic rate limit (i.e., $q_{elf} = nq_f$ with $n \geq 1$), the EUR for hyperbolic decline becomes:

$$EUR = \frac{2\sqrt{t_{elf}}}{m}\left[1 + \frac{1}{1-b}(1 - n^{b-1})\right] \tag{22}$$

Using Eq. (22), it can be shown that the ratio between EUR values obtained for two different values of decline exponent depends on the value of n, given that the two decline exponents are specified. When EUR is being calculated based upon economic limit, Eq. (22) can be used to investigate the sensitivity of EUR to decline exponent.

CONCLUSIONS

This paper applied the simplified forecasting method of Nobakht et al.[1] to study the sensitivity of expected ultimate recovery (EUR) to decline exponent used after the end of linear flow. This is important for reserve evaluation because of uncertainty in decline exponent due to factors like desorption and heterogeneity in completion. It was shown that for gas production under constant flowing pressure in a volumetric reservoir, at some point during depletion the decline exponent starts to deviate from 0.5. The time at which this deviation happens is almost $t = 6t_{elf}$ for the reservoir geometry shown in Fig. 1, where t_{elf} is the duration of linear flow. Using some assumptions, it was shown that ignoring the gradual decrease in b-value after $t = 6t_{elf}$ will not practically affect the EUR. Finally, the sensitivity of EUR to b-value is studied for both time-based and economic limit-based forecasts. It is found that for two different specified values of decline exponent, the ratio between their EURs depends on the ratio of economic life of the well to the duration of linear flow for time-based forecast and the ratio of the rate at the end of linear flow to the economic rate limit for economic limit-based forecast.

ACKNOWLEDGEMENTS

The authors would like to thank ConocoPhillips for their support of this research. Chris Clarkson would like to acknowledge Encana for support of his Chair position in Unconventional Gas at the University of Calgary, Department of Geoscience. Finally, both authors would like to thank Fekete Associates Inc., particularly Louis Mattar, for fruitful discussions on the subject of rate-transient analysis.

REFERENCES

[1] Nobakht, M., Mattar, L., Moghadam, S., & Anderson, D. M. (2010). Simplified Yet Rigorous Forecasting of Tight/Shale Gas Production in Linear Flow. *Paper SPE 133615 presented at the SPE Western Regional Meeting, Anaheim, California, 27–29 May*. DOI: 10.2118/133615-MS.

[2] Cipolla, C. L., Williams, M. J., Weng, X., & Maxwell, S. (2010). Hydraulic Fracture Monitoring to Reservoir Simulation: Maximizing Value. *Paper SPE 133877 presented at the SPE Annual Technical Conference and Exhibition, Florence, Italy, 19–22 September*. DOI:

10.2118/133877-MS.
[3] Arps, J. J. (1945). Analysis of Decline Curves. *Trans., AIME*, *160*, 228–247.
[4] Stright, D. H., & Gordon, J. I. (1983). Decline Curve Analysis in fractured Low Permeability Gas Wells in the Piceance Basin. *Paper SPE 11640 presented at the SPE/DOE Low Permeability Gas Reservoirs Symposium, Denver, Colorado, 14–16 March*. DOI: 10.2118/11640-MS.
[5] Maley, S. (1985). The Use of Conventional Decline Curve Analysis in Tight Gas Well Applications. *Paper SPE 13898 presented at the SPE/DOE Low Permeability Gas Reservoirs Symposium, Denver, Colorado, 19–22 March*. DOI: 10.2118/13898-MS.
[6] Hale, B. W. (1986). Analysis of Tight Gas Well Production Histories in the Rocky Mountains. *SPE Production Engineering*, *1*(4), 310–322. SPE-11639-PA. DOI: 10.2118/11639-PA.
[7] Wattenbarger, R. A., El-Banbi, A. H., Villegas, M. E., & Maggard, J. B. (1998). Production Analysis of Linear Flow into Fractured Tight Gas Wells. *Paper SPE 39931 presented at SPE Rocky Mountain Regional/Low Permeability Reservoirs Symposium and Exhibition, Denver, Colorado, 5–8 April*. DOI: 10.2118/39931-MS.
[8] Kupchenko, C. L., Gault, B. W., & Mattar, L. (2009). Tight Gas Production Performance Using Decline Curves. *Paper SPE 114991 presented at the CIPC/SPE Gas Technology Symposium, Calgary, Alberta, 16–19 June*. DOI: 10.2118/114991-MS.
[9] Ilk, D., Rushing, J. A., Perego, A. D., & Blasingame, T. A. (2008). Exponential vs. Hyperbolic Decline in Tight Gas Sands — Understanding the Origin and Implications for Reserve Estimates Using Arps' Decline Curves. *Paper SPE 116731, presented at the Annual Technical Conference and Exhibition, Denver, Colorado, 21–24 September*. DOI: 10.2118/116731-MS.
[10] Valkó, P. P. (2009). Assigning Value to Stimulation in the Barnett Shale: A Simultaneous Analysis of 7000 Plus Production Histories and Well Completion Records. *Paper SPE 119369 presented at SPE Hydraulic Fracturing Technology Conference, The Woodlands, Texas, 19–21 January*. DOI: 10.2118/119369-MS.
[11] Ambrose, R. J., Clarkson, C. R., Youngblood, J., Adams, R., Nguyen, P., Nobakht, M., & Biseda, B. (2011). Life-Cycle Decline Curve Estimation for Tight/Shale Gas Reservoirs. *Paper SPE 140519 presented at the SPE Hydraulic Fracturing Technology Conference and Exhibition, The Woodlands, Texas, 24–26 January*. DOI: 10.2118/140519-MS.
[12] Nobakht, M., Ambrose, R. J., & Clarkson, C. R. (2011). Effect of Heterogeneity in a Horizontal Well With Multiple Fractures on the Long-Term Forecast in Shale Gas Reservoirs. *Paper CSUG/SPE 149400 presented at the Canadian Unconventional Resources Conference, Calgary, Alberta, Canada, 15–17 November*. DOI: 10.2118/149400-MS.
[13] Okuszko, K. E., Gault, B. W., & Mattar, L. (2007). Production Decline Performance of CBM Wells. *Paper CIPC 2007-78, presented at Canadian International Petroleum Conference, Calgary, Alberta, 12–14 June*. DOI: 10.2118/2007-78.
[14] Nobakht, M., & Clarkson, C. R. (2011). A New Analytical Method for Analyzing Production Data from Shale Gas Reservoirs Exhibiting Linear Flow: Constant Pressure Production. *Paper SPE 143989 presented at the North American Unconventional Gas Conference, The Woodlands, Texas, 12–16 June*. DOI: 10.2118/143989-MS.
[15] Nobakht, M., & Clarkson, C. R. (2011). A New Analytical Method for Analyzing Production Data from Shale Gas Reservoirs Exhibiting Linear Flow: Constant Rate Production. *Paper SPE 143990 presented at the North American Unconventional Gas Conference, The Woodlands, Texas, 12–16 June*. DOI: 10.2118/143990-MS.
[16] Ibrahim, M., & Wattenbarger R. A. (2005). Rate Dependence of Transient Linear Flow in Tight Gas Wells. *Paper CIPC 2005-057 presented at Canadian International Petroleum Conference, Calgary, Alberta, 7–9 June*. DOI: 10.2118/2005-057.
[17] Ibrahim, M., & Wattenbarger R. A. (2006). Analysis of Rate Dependence in Transient Linear Flow in Tight Gas Wells. *Paper SPE 100836 presented at the Abu Dhabi International Petroleum Exhibition and Conference, Abu Dhabi, UAE, 5–8 November*. DOI: 10.2118/100836-MS.
[18] Nobakht, M., & Clarkson, C. R. (2011). Estimation of Contacted and Original Gas-in-Place for Low Permeability Reservoirs Exhibiting Linear Flow. *Paper CSUG/SPE 149398 presented at the the Canadian Unconventional Resources Conference, Calgary, Alberta, Canada, 15–17 November*. DOI: 10.2118/149398-MS.

APPENDIX A: Duration of Linear Flow and Development of Figure 4

When the well is producing under constant flowing pressure in the reservoir geometry shown in Fig. 1, the distance of investigation, y, can be obtained from the following equation during the linear flow period[7]:

$$y = 0.159\sqrt{\frac{kt}{(\phi\mu_g c_t)_i}} \tag{A-1}$$

According to this equation, the end of linear flow is given by:

$$\frac{y_e}{2} = 0.159\sqrt{\frac{kt_{elf}}{(\phi\mu_g c_t)_i}}, \tag{A-2}$$

where y_e is reservoir length and t_{elf} is the duration of linear flow. Eq. (A-2) can be rewritten as follows:

$$t_{elf} = \left(\frac{y_e\sqrt{(\phi\mu_g c_t)_i}}{2\times 0.159\sqrt{k}}\right)^2 \tag{A-3}$$

Using t_{elf} calculated from Eq. (A-3) in Eq. (7), t_{Dye} at the end of linear, $(t_{Dye})_{elf}$, becomes:

$$(t_{Dye})_{elf} = \frac{0.00633kt_{elf}}{\phi\mu c_t y_e^2} = 0.0625 \tag{A-4}$$

In other words, $t_{Dye} = 0.0625$ at the end of linear flow. Note that this value is different from t_{Dye}=0.25 Wattenbarger et al.[7] derived simply because in their work y_e was half of reservoir length, whereas in this study y_e is the reservoir length.

To generate the type curve shown in Fig. 4 for the reservoir geometry in Fig. 1, we used the following equation, which is linear flow solution for constant flowing pressure, for $t_{Dye} \le 0.0625$ (i.e., duration of linear flow).

$$\frac{1}{q_{Dd}} = \pi\sqrt{\pi t_{Dye}} \tag{A-5}$$

For $t_{Dye} \ge 0.0625$ (i.e., boundary-dominated flow), we used the following equation (with $b = 0.5$), which is the extension of Nobakht et al.[1] method in dimensionless form:

$$q_{Dd} = \frac{(q_{Dd})_{elf}}{\left[1 + bD_{elf}(t_{Dye} - (t_{Dye})_{elf})\right]^{1/b}} \tag{A-6}$$

Here, $(q_{Dd})_{elf}$ is value of q_{Dd} at $t_{Dye} = (t_{Dye})_{elf} = 0.0625$ ($(q_{Dd})_{elf} \approx 0.718$) and D_{elf} is as follows:

$$D_{elf} = \frac{1}{2(t_{Dye})_{elf}} = 8 \tag{A-7}$$

APPENDIX B: Calculation of Volume Produced During Different Time Intervals

For the reservoir geometry shown in Fig. 1, the end of linear flow, t_{elf}, is[1,7] :

$$t_{elf} = \left[\frac{Ah(\phi\mu_g c_t)_i m\ (p_{pi} - p_{pwf})}{200.6T}\right]^2 \tag{B-1}$$

Combining Eqs. (B-1), (8)–(11) results in:

$$\sqrt{t_{elf}} = \frac{Ah\phi\mu_{gi}}{200.6T}\frac{Sg}{p_i}m\frac{p_i^2}{\mu_{gi}} = \frac{Ah\phi S_g}{200.6}\frac{p_i}{T}m \tag{B-2}$$

Using the definition of gas formation volume factor $B_{gi} = \frac{0.0282Z_iT}{p_i}$ with $Z_i = 1$ (ideal gas assumption),

$$\frac{p_i}{T} = \frac{0.0282}{B_{gi}} \tag{B-3}$$

Combining Eqs. (B-2) and (B-3) and using the definition of $OGIP = 0.001\frac{Ah\phi S_g}{B_{gi}}$ ($OGIP$ is in Mscf),

$$\frac{\sqrt{t_{elf}}}{m} == \frac{Ah\phi S_g}{200.6}\frac{0.0282}{B_{gi}} = 0.141OGIP \tag{B-4}$$

Using the value of $\frac{\sqrt{t_{elf}}}{m}$ from Eq. (B-4) into Eq. (13),

$$Q_{elf} = 0.282OGIP \tag{B-5}$$

The rate at $t = 6t_{elf}$, can be calculated by combing Eqs. (3) and (5) (with $b' = 0$, i.e., zero intercept on inverse gas rate versus square root of time plot):

$$q_{6elf} = 0.198q_{elf} \tag{B-6}$$

Using hyperbolic decline with $b = 0.5$ between $t = t_{elf}$ and $t = 6t_{elf}$, the decline rate at $t = 6t_{elf}$ can be calculated using:

$$\frac{D_{6elf}}{D_{elf}} = \left(\frac{q_{6elf}}{q_{elf}}\right)^{0.5} \tag{B-7}$$

Combining Eqs. (B-6) and (B-7),

$$D_{6elf} = 0.444D_{elf} \tag{B-8}$$

The volume produced after $t = 6t_{elf}$ using hyperbolic decline with $b = 0.5$ and exponential decline can be calculated using Eqs. (B-9) and (B-10), respectively:

$$\Delta Q = \frac{q_{6elf}^b}{(1-b)D_{6elf}}\left(q_{6elf}^{1-b} - q_f^{1-b}\right) \tag{B-9}$$

$$\Delta Q = \frac{q_{6elf} - q_f}{D_{6elf}} \tag{B-10}$$

Using $q_f = 0$, Eqs. (B-9) and (B-10) will change to:

$$\Delta Q = \frac{2q_{6elf}}{D_{6elf}} = \frac{1.784q_{elf}}{D_{elf}} \tag{B-11}$$

$$\Delta Q = \frac{q_{6elf}}{D_{6elf}} = \frac{0.892q_{elf}}{D_{elf}} \tag{B-12}$$

Using Eqs. (2), (3) and (B-4),

$$\Delta Q = 0.246 OGIP \tag{B-13}$$

$$\Delta Q = 0.123 OGIP \tag{B-14}$$

It can be concluded from Eqs. (B-13) and (B-14) that 25% of the total original gas-in-place is produced after $t = 6t_{elf}$ using hyperbolic decline with $b = 0.5$, whereas 12% of the total original gas-in-place is produced after $t = 6t_{elf}$ using exponential decline.

